JOURNAL OF MATERIALS SCIENCE 11 (1976) 1305–1309

Phase relationships in the system Si_3N_4-Y_2O_3-SiO_2

R. R. WILLS
Systems Research Laboratories, Inc., 2800 Indian Ripple Road, Dayton, Ohio, USA

S. HOLMQUIST*
Universal Technology Corporation, 1656 Mardon Drive, Dayton, Ohio, USA

J. M. WIMMER, J. A. CUNNINGHAM
Air Force Materials Laboratory, Wright Patterson Air Force Base, Ohio, USA

Examination of compositions in the system Si_3N_4–Y_2O_3–SiO_2 using sintered samples revealed the existence of two regions of melting and three silicon yttrium oxynitride phases. The regions of melting occur at ~1600° C at high SiO_2 concentrations (~13 mol % Si_3N_4 + 19 mol % Y_2O_3 + 68 mol % SiO_2) and at 1650° C at high Y_2O_3 concentrations (25 mol % Si_3N_4 + 75 mol % Y_2O_3). Two ternary phases $4Y_2O_3 \cdot SiO_2 \cdot Si_3N_4$ and $10Y_2O_3 \cdot 9SiO_2 \cdot Si_3N_4$ and one binary phase $Si_3N_4 \cdot Y_2O_3$ were observed. The $4Y_2O_3 \cdot SiO_2 \cdot Si_3N_4$ phase has a monoclinic structure (a = 11.038 Å, b = 10.076 Å, c = 7.552 Å, β = 108° 40′) and appears to be isostructural with silicates of the wohlerite cuspidine series. The $10Y_2O_3 \cdot 9SiO_2 \cdot Si_3N_4$ phase has a hexagonal unit cell (a = 7.598 Å c = 4.908 Å). Features of the Si_3N_4–Y_2O_3–SiO_2 systems are discussed in terms of the role of Y_2O_3 in the hot-pressing of Si_3N_4, and it is suggested that Y_2O_3 promotes a liquid-phase sintering process which incorporates dissolution and precipitation of Si_3N_4 at the solid–liquid interface.

1. Introduction

Hot-pressed Si_3N_4 is one of the leading candidate materials for components in high-temperature gas turbines. High-strength and fully dense bodies are generally obtained by the addition of up to 5 wt % MgO to the α-Si_3N_4 starting powder [1]. The MgO promotes the formation of a liquid phase [2], which enables the material to be hot pressed to full density. However, the high-temperature strength of the material sharply decreases above 1000° C due to the presence of the glassy grain-boundary phase formed by the reaction of the MgO additive with SiO_2 and metal impurities, both of which are associated with the α-Si_3N_4 powder [3, 4]. Improvements in high-temperature strength have recently been obtained either by increasing the vicosity of the grain-boundary phase as in the Norton Co NC132 (Norton Co, Worcester Mass. 01606, USA) grade Si_3N_4 or by achieving a more refractory grain-boundary phase. The latter approach has been adopted by Gazza [5, 6] and by Mazdiyasni and Cooke [7] who investigated the effect of rare-earth oxide additions on the hot-pressing of Si_3N_4. Gazza [5] found that the addition of 1 to 3.3 wt % Y_2O_3 yielded hot-pressed bodies with a four-point bend strength of 400 MN m^{-2} (58 000 psi) to 476 MN m^{-2} (69 000 psi) at 1315° C. However, the highest strengths are obtained only with Y_2O_3 concentrations greater than 10 wt %. Torti [8] has reported three-point bend strengths of 743 MN m^{-2} (107 000 psi) at 1375° C for Si_3N_4 with 13 wt % Y_2O_3 and 733 MN m^{-2} (106 000 psi) for 16 wt % Y_2O_3.

It has been shown that when Y_2O_3 is used as

* Visiting Research Associate at Aerospace Research Laboratories, Wright-Patterson Air Force Base, Ohio 45433, under Contract No. F33615–73–C–4155 when this work was carried out.

the hot-pressing additive, the high-temperature properties are controlled by a refractory grain-boundary phase of composition $Si_3N_4 \cdot Y_2O_3$ [9, 10], and it has been suggested [9] that densification occurs by way of a transient silicon–yttrium–oxynitride melt, during the hot-pressing cycle. However, the possible role of the surface SiO_2 on the Si_3N_4 powder was not considered in this explanation. The present investigation was thus directed toward determining the main features of the Si_3N_4–Y_2O_3–SiO_2 system in an effort to understand the densification of Si_3N_4.

2. Experimental

The main features of the system were established using 3 g discs, $\frac{3}{4}$ in. diameter, made by the cold compaction of Si_3N_4 (Advanced Materials Engineering Ltd, Gateshead, UK), Y_2O_3 (Kerr McGee Chemical Corp, Oklahoma City, Oklahoma) and SiO_2 (Atomergic Chemetals Co, Long Island, N.Y. 11514). The mean particle size of all powders was 2 to 6 μm. Larger samples (~20g) used primarily to obtain thermal-expansion data, were prepared by isostatic pressing at 140 MN m^{-2} (20 000 psi). The powders were mixed in propan–2–ol using a Waring blender. Samples were supported on a bed of BN powder during firing in a N_2 atmosphere at 1575 to 1750° C for 1 h. Before the N_2 entered the resistance-heated alumina-tube furnace, it was passed through ascartite, magnesium perchlorate, and heated copper/copper oxide catalytic pellets to remove carbon dioxide, water, hydrocarbons, and oxygen. The weight loss for the smaller samples during firing was ~2%, whereas for the larger samples it was ~1%. The sintered discs were examined as powders using a recording X-ray diffractometer (Cu$K\alpha$). Standard metallographic and SEM techniques were employed to examine microstructural features.

3. Results and discussion

3.1. Phase relationships

The main features of the system are shown in Fig. 1. Solid-state equilibria at 1700° C were explored by establishing compatability triangles according to the "clear cross" principle [11, 12] The yttrium silicate, $2Y_2O_3 \cdot 3SiO_2$ found in the Y_2O_3–SiO_2 phase diagram by Toropov and Bondar [13] was not observed and consequently is not shown. There is no tie line between $Si_3N_4 \cdot Y_2O_3$ and Y_2O_3 and, therefore, it is likely that a tie line exists between the ternary phase $4Y_2O_3 \cdot SiO_2 \cdot Si_3N_4$ and a YN–rich phase. YN along with Si_3N_4, SiO_2, and Y_2O_3, constitutes one plane in the tetrahedron Si–Y–O–N.

3.2. Melting

In the triangle SiO_2–$Y_2O_3 \cdot 2SiO_2$–Si_2N_2O, several samples exhibited bloating. The minimum temperature at which this was observed was ~1600° C in the region of composition 13 mol% Si_3N_4 + 19 mol% Y_2O_3 + 68 mol% SiO_2. Along the Y_2O_3–SiO_2 binary, the lowest liquidus temperature is 1660° C at 72 mol% SiO_2 + 28 mol % Y_2O_3 [13]. It would thus appear that Si_3N_4 dissolves in this liquid and lowers the liquidus temperature. In the lower part of the diagram, melting was observed at 1650° C in the region of composition 25 mol% Si_3N_4 + 75 m% Y_2O_3.

TABLE I Observed and calculated diffraction data for $Si_3N_4 \cdot Y_2O_3$

hkl	*d* (Å)	Relative intensity	Q_{obs}	Q_{calc}
1 1 0	5.400	8	0.0343	0.0346
0 0 1	4.951	11	0.0408	0.0415
2 0 0	3.830	7	0.0682	0.0693
1 1 1	3.644	15	0.0753	0.0762
1 2 0	3.411	9	0.0859	0.0866
2 0 1	3.015	25	0.1100	0.1108
1 2 1	2.794	100	0.1281	0.1281
2 2 0	2.696	5	0.1376	0.1386
0 0 2	2.459	9	0.1654	0.1660
1 3 0	2.408	17	0.1724	0.1732
2 2 1	2.359	4	0.1797	0.1801
1 0 2	2.336	3	0.1832	0.1833
3 0 1	2.252	3	0.1978	0.1974
1 1 2	2.230	3	0.2011	0.2006
1 3 1	2.159	4	0.2145	0.2147
2 0 2	2.065	3	0.2345	0.2353
1 2 2	1.991	19	0.2523	0.2526
4 0 0	1.897	8	0.2779	0.2772
4 1 0	1.843	7	0.2944	0.2945
2 2 2	1.812	12	0.3046	0.3046
3 3 0	1.792	10	0.3114	0.3118
4 1 1	1.726	12	0.3357	0.3359
3 1 2	1.717	17	0.3392	0.3392
4 2 0	1.699	5	0.3464	0.3464
3 3 1	1.682	9	0.3535	0.3533
2 1 3	1.474	12	0.4603	0.4602
3 3 2	1.449	5	0.4763	0.4778
5 2 1	1.359	9	0.5414	0.5438

Tetragonal $a = 7.598$ Å, $c = 4.908$ Å

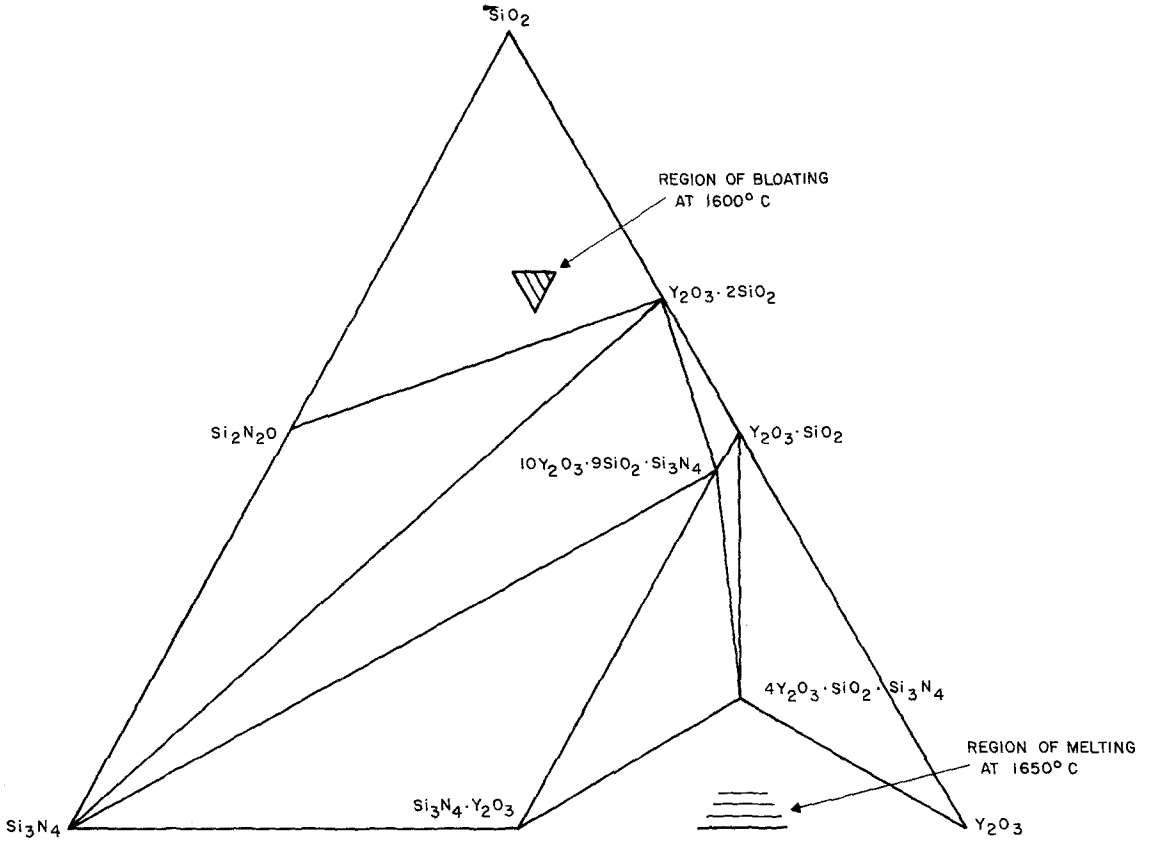

Figure 1 The system Si_3N_4–Y_2O_3–SiO_2 showing solid–solid equilibria at 1700° C.

3.3. Phase identification

The diffraction patterns for three recently reported [9, 10] silicon–yttrium–oxynitride phases were confirmed and established in more detail. Microstructural analysis of the sintered discs suggested that the probable compositions of these phases were $Si_3N_4 \cdot Y_2O_3$, $Si_3N_4 \cdot 3Y_2O_3$, and $10Y_2O_3 \cdot 9SiO_2 \cdot Si_3N_4$. The exact composition of the second oxynitride was difficult to establish, but since electron microprobe analysis gave the Y/Si ratio as 2:1, $Si_3N_4 \cdot 3Y_2O_3$ was considered to be the probable composition. After indexing of the diffraction pattern, the correct composition of this phase is considered to be $4Y_2O_3 \cdot SiO_2 \cdot Si_3N_4$ or $Y_4Si_2O_7N_2$. Thus, the Si_3N_4–Y_2O_3–SiO_2 system contains two ternary phases and four binary phases.

The powder pattern of the binary compound $Si_3N_4 \cdot Y_2O_3$ can be indexed on the basis of a tetragonal cell (Table I). The lattice parameters $a = 7.598$ Å, $c = 4.908$ Å agree closely with those found by Tsuge *et al.* [15] ($a = 7.603$ Å, $c = 4.910$ Å) and by Rae *et al.* [10] ($a = 7.597$ Å, $c = 4.908$ Å). The latter group has shown that $Si_3N_4 \cdot Y_2O_3$ is isostructural with the melilite silicates; Akermanite $Ca_2MgSi_2O_7$ and Gehlenite $Ca_2Al(SiAlO_7)$ and have stated that the oxynitride has a complete range of solid solubility with both silicates.

The powder pattern of the ternary phase $10Y_2O_3 \cdot 9SiO_2 \cdot Si_3N_4$ was indexed on the basis of a hexagonal unit cell having lattice parameters $a = 9.436$ Å, $c = 6.822$ Å. Table II gives the the diffraction lines and illustrates the good agreement between the calculated and observed Q values ($Q = 4 \sin^2\theta/\lambda^2$). This compound corresponds to the H phase of Rae *et al.* [10]; Thompson [15] has suggested that it is isostructural with fluoroapatite $Ca_5(PO_4)_3F$ (hexagonal $a = 9.368$ Å $c = 6.881$ Å), and thus may be represented by the formula $Y_5(SiO_4)_3N$. This oxynitride was found to be stable up to ~1750° C in a N_2 atmosphere whereupon it slowly dissociated to Y_2O_3 and $Y_2O_3 \cdot SiO_2$.

The second ternary phase, $4Y_2SiO_2 \cdot Si_3N_4$, was determined to have a monoclinic unit cell with lattice parameters $a = 11.038$ Å, $b = 10.076$ Å, $c = 7.552$ Å, $\beta = 108°46'$. The d spacings and

TABLE II Observed and calculated diffraction data for $10Y_2O_3 \cdot 9SiO_2 \cdot Si_3N_4$

hkl	*d* (Å)	Relative intensity	Q_{obs}	Q_{calc}
1 1 0	4.741	4	0.0445	0.0445
2 0 0	4.101	26	0.0595	0.0599
1 1 1	3.896	10	0.0659	0.0664
0 0 2	3.411	15	0.0859	0.0859
1 0 2	3.145	36	0.1011	0.1009
2 1 0	3.086	35	0.1050	0.1048
2 1 1	2.811	100	0.1265	0.1263
1 1 2	2.760	65	0.1312	0.1308
3 0 0	2.724	41	0.1347	0.1347
2 0 2	2.615	10	0.1462	0.1458
3 0 1	2.526	2	0.1567	0.1562
2 2 0	2.353	1	0.1806	0.1796
2 1 2	2.284	4	0.1917	0.1907
3 1 0	2.262	7	0.1954	0.1946
2 2 1	2.225	6	0.2019	0.2011
3 1 1	2.143	3	0.2177	0.2161
3 0 2	2.122	7	0.2220	0.2207
4 0 0	2.038	12	0.2407	0.2396
2 0 3	1.983	2	0.2543	0.2533
2 2 2	1.933	40	0.2676	0.2656
3 1 2	1.880	17	0.2829	0.2806
3 2 0	1.868	6	0.2865	0.2845
2 1 3	1.824	41	0.3005	0.2939
3 2 1	1.802	18	0.3079	0.3059
4 1 0	1.776	27	0.3170	0.3144
4 0 2	1.746	25	0.3280	0.3255
0 0 4	1.698	16	0.3468	0.3438

Hexagonal $a = 9.436$ Å, $c = 6\ 822$ Å

observed and calculated Q values are given in Table III. Rae *et al.* [10], called this phase the *J* phase. Comparison of the lattice parameters of this phase with those of the silicates suggests that this phase is probably isostructural with the silicates of the wohlerite–cuspidine series. Cuspidine ($Ca_4Si_2O_7F_2$) has the lattice parameters $a = 10.35$ Å, $b = 10.43$ Å, $c = 7.55$ Å, $\beta = 110° 4'$. The composition of this phase may, therefore, be represented by the formula $Y_4Si_2O_7N_2$. In contrast to $Y_5(SiO_4)_3N$, $Y_4Si_2O_7N_2$ appeared to be stable at 1750° C under the same atmosphere.

3.4. Thermal expansion of the silicon yttrium oxynitrides

The linear coefficients of thermal expansion of these compounds as determined by a dilatometric technique are high relative to Si_3N_4 (see Table IV) which suggests that the presence of one or more of these phases in hot-pressed Si_3N_4 could influence its thermal and mechanical properties.

TABLE III Observed and calculated diffraction data for $4Y_2O_3 \cdot SiO_2 \cdot Si_3N_4$

hkl	*d* (Å)	Relative intensity	Q_{obs}	Q_{calc}
1 1 0	7.248	12	0.0190	0.0190
0 2 0	5.034	2	0.0395	0.0394
1 2 0	4.525	15	0.0488	0.0485
2 2 0	3.644	5	0.0753	0.0759
1 3 0	3.195	22	0.0980	0.0978
1 3 1	3.055	100	0.1071	0.1088
0 2 2	2.919	15	0.1174	0.1174
3 2 0	2.864	31	0.1219	0.1215
2 3 0	2.828	54	0.1250	0.1251
4 0 1	2.736	7	0.1336	0.1317
$\bar{3}$ 1 1	2.712	7	0.1360	0.1368
4 0 0	2.619	8	0.1458	0.1459
0 4 0	2.519	16	0.1576	0.1576
2 0 3 ($\bar{2}$ 3 1)	2.499	11	0.1601	0.1612 (0.1615)
$\bar{3}$ 2 1, 4 1 2	2.453	6	0.1662	0.1662
3 1 3	2.284	6	0.1917	0.1913
2 4 0	2.273	5	0.1936	0.1941
$\bar{3}$ 3 1	2.149	4	0.2165	0.2156
3 4 0	2.042	10	0.2398	0.2397
$\bar{5}$ 2 1	2.029	7	0.2429	0.2447
$\bar{3}$ 2 2	1.979	15	0.2553	0.2501
$\bar{2}$ 5 0	1.890	15	0.2799	0.2827
$\bar{3}$ 4 1	1.875	7	0.2844	0.2845
$\bar{2}$ 4 2 (6 0 2)	1.815	14	0.3056	0.3058 (0.3050)
6 1 1	1.805	14	0.3069	0.3071
$\bar{2}$ 5 1	1.773	5	0.3181	0.3191
3 5 1	1.760	6	0.3228	0.3225
6 0 0, 3 5 0	1.749	6	0.3269	0.3284
6 1 0	1.717	14	0.3392	0.3382
$\bar{6}$ 0 1	1.588	5	0.3966	0.3985
0 3 4	1.576	11	0.4026	0.4004
$\bar{6}$ 1 1	1.564	8	0.4088	0.4084
$\bar{2}$ 6 1	1.531	6	0.4266	0.4275
3 6 1	1.526	5	0.4294	0.4308
3 6 0	1.517	5	0.4345	0.4337

Monoclinic $a = 11.038$ Å; $b = 10.076$ Å; $c = 7.552$ Å; $\beta = 108.46°$

TABLE IV Thermal expansion of the silicon yttrium oxynitrides

Compound	Linear expansion coefficient (20 to 1000° C)
$Si_3N_4 \cdot Y_2O_3$	5.8×10^{-6} °C^{-1}
$4Y_2O_3 \cdot SiO_2 \cdot Si_3N_4$	6.6×10^{-6} °C^{-1}
$10Y_2O_3 \cdot 9SiO_2 \cdot Si_3N_4$	8.2×10^{-6} °C^{-1}

3.5. Role of Y_2O_3 and SiO_2 in the hot-pressing of Si_3N_4

The probable explanation of the role of the Y_2O_3 additive in the hot-pressing of Si_3N_4 is that the initial reaction below 1600° C results in the formation of a SiO_2-rich Si_3N_4–SiO_2–Y_2O_3 liquid at

the grain boundaries which acts as an initial densification aid. Since the availability of SiO_2 is limited, further reaction results in the formation of a liquid of approximate composition 25 mol% Si_3N_4 + 75 mol% Y_2O_3 at ~1650°C, and this melt is probably the principal liquid phase present during the hot-pressing cycle, enabling the Si_3N_4 to be pressed to low porosity levels. During this stage of the process, the interaction of the melt with the Si_3N_4 grains produces the final grain-boundary oxynitride phase, $Si_3N_4 \cdot Y_2O_3$. Incomplete reaction can be readily detected by the appearance of the phase $4Y_2O_3 \cdot Si_3N_4 \cdot SiO_2$ in the final product which precipitates out of the melt during cooling (see Fig. 1).

The high-temperature strength of the resulting ceramic bodies is due to the presence of $Si_3N_4 \cdot Y_2O_3$ as the grain-boundary phase. Tsuge *et al.* [14], have estimated that it does not become liquid until ~1830°C. Furthermore, this phase has the ability to dissolve small amounts of SiO_2 and appreciable amounts of metal impurities [10] which might otherwise form low-softening-point glassy phases. Optimum Y_2O_3 additions (> 10 w%) are thus associated with promoting the formation of this phase.

The role of metal impurities has not been fully established, but it is likely that they affect the liquid phases that form during the pressing cycle and, hence, influence the ultimate porosity levels and strength of the ceramic body. For example, Huseby and Petzow [16] examined the influence of 17 additives including Y_2O_3 on hot-pressed Si_3N_4 and found that complete densification could be achieved with only one of the two α-Si_3N_4 powders used. Furthermore, Norton Co Y_2O_3-based Si_3N_4 HX415 contains WSi_2 resulting from the reaction of WC (from the ball billing) with Si_3N_4. A complete understanding of the densification and mechanical properties of hot-pressed Si_3N_4 produced using Y_2O_3 as the densifying additive cannot, therefore, be achieved until the effect of metal impurities is known. However, the liquid-phase sintering, dissolution of Si_3N_4, and precipitation of solid material observed in the Si_3N_4–Y_2O_3–SiO_2 system strongly suggest that Y_2O_3 acts in a manner similar to MgO [2] and Al_2O_3 [17] in the hot-pressing of Si_3N_4 in facilitating liquid-phase densification and a solid–liquid–solid $\alpha \rightarrow \beta$ transformation mechanism.

Acknowledgement

This work was supported in part under USAF Contract F33615-75-C-1005.

References

1. G. C. DEELEY, J. M. HERBERT and N. C. MOORE, *Powder Met.* 8 (1961) 145.
2. P. DREW and M. H. LEWIS, *J. Mater. Sci.* 9 (1974) 261.
3. D. W. RICHERSON, *Amer. Ceram. Soc. Bull.* 52 (1973) 560.
4. F. F. LANGE and J. L. ISKOE, "Proceedings of the Second Army Materials Technology Conference: Ceramics for High Performance Applications," (Brook Hill, Chestnut Hill, Massachusetts, 1974) p. 223.
5. G. E. GAZZA, *J. Amer. Ceram. Soc.* 56 (1973) 602.
6. G. E. GAZZA, D. R. MESSIER and P. WONG, "Recent Developments in Processing Si_3N_4," presented at the Third Materials Conference on Turbine Applications, Ann Arbor, Michigan, 30 October to 1 November, 1974.
7. K. S. MAZDIYASNI and C. M. COOKE, *J. Amer. Ceram. Soc.* 57 (1974) 536.
8. M. L. TORTI, "The Effects of Fabrication Procedures Upon Mechanical Properties of Si_3N_4 and SiC Turbine Components," presented at the Third Materials Conference on Turbine Applications, Ann Arbor, Michigan, 30 October to 1 November, 1974.
9. R. R. WILLS, *J. Amer. Ceram. Soc.* 57 (1974) 459.
10. A. W. J. M. RAE, D. P. THOMPSON, N. J. PIPKIN and K. H. JACK, *Special Ceramics* 6 (1975) 347.
11. F. N. RHINES, "Phase Diagrams in Metallurgy" (McGraw Hill, New York, 1956) p. 203.
12. W. R. FOSTER, *Bull. Amer. Ceram. Soc.* 30 (1951) 267, 291.
13. N. A. TOROPOV and I. A. BONDAR, *Izv. Akad. Nauk, SSR, Otd. Khim. Nauk* 4 (1961) 544, 1372.
14. A. TSUGE, H. KUDO and K. KOMEYA, *J. Amer. Ceram. Soc.* 57 (1974) 269.
15. D. P. THOMPSON, *Special Ceramics* 6 (1975) 358.
16. I. C. HUSEBY and C. PETZOV, *Powder Met. Int.* 1 (1974) 17.
17. P. DREW and M. H. LEWIS, *J. Mater. Sci.* 9 (1974) 1833.

Received 8 October and accepted 17 November 1975.